Journal of Cellular Physiology

Cell Surface Human Airway Trypsin-Like Protease Is Lost During Squamous Cell Carcinogenesis

MICHAEL J. DUHAIME,[1] KHALIPH O. PAGE,[1] FAUSTO A. VARELA,[1] ANDREW S. MURRAY,[1,2,3] MICHAEL E. SILVERMAN,[1] GINA L. ZORATTI,[2] AND KARIN LIST[1,2]*

[1]*Department of Pharmacology, Wayne State University School of Medicine and Barbara Ann Karmanos Cancer Institute, Detroit, Michigan*

[2]*Department of Oncology, Wayne State University School of Medicine and Barbara Ann Karmanos Cancer Institute, Detroit, Michigan*

[3]*Department of Cancer Biology Graduate Program, Wayne State University School of Medicine and Barbara Ann Karmanos Cancer Institute, Detroit, Michigan*

Cancer progression is accompanied by increased levels of extracellular proteases that are capable of remodeling the extracellular matrix, as well as cleaving and activating growth factors and receptors that are involved in pro-cancerous signaling pathways. Several members of the type II transmembrane serine protease (TTSP) family have been shown to play critical roles in cancer progression, however, the expression or function of the TTSP Human Airway Trypsin-like protease (HAT) in carcinogenesis has not been examined. In the present study we aimed to determine the expression of HAT during squamous cell carcinogenesis. HAT transcript is present in several tissues containing stratified squamous epithelium and decreased expression is observed in carcinomas. We determined that HAT protein is consistently expressed on the cell surface in suprabasal/apical layers of squamous cells in healthy cervical and esophageal epithelia. To assess whether HAT protein is differentially expressed in normal tissue versus tissue in different stages of carcinogenesis, we performed a comprehensive immunohistochemical analysis of HAT protein expression levels and localization in arrays of paraffin embedded human cervical and esophageal carcinomas compared to the corresponding normal tissue. We found that HAT protein is expressed in the non-proliferating, differentiated cellular strata and is lost during the dedifferentiation of epithelial cells, a hallmark of squamous cell carcinogenesis. Thus, HAT expression may potentially be useful as a marker for clinical grading and assessment of patient prognosis in squamous cell carcinomas.

J. Cell. Physiol. 231: 1476–1483, 2016.

During the last two decades, cell surface proteases belonging to the type II transmembrane serine protease (TTSP) family, have emerged as enzymes with important functions in epithelial biology and pathology, including cancer (Hobson et al., 2004; Szabo and Bugge, 2008, 2011; Bugge et al., 2009; List, 2009; Antalis et al., 2010).

The human TTSP family encompasses 17 known members in humans that all contain an N-terminal transmembrane domain, a C-terminal extracellular serine protease domain and a "stem region" that contain various types, combinations, and numbers of conserved domains. Human Airway Trypsin-like protease (HAT) has the simplest domain configuration, where the stem region contains a single sea urchin sperm protein, enteropeptidase, agrin (SEA) domain (Szabo and Bugge, 2011). HAT belongs to the HAT/DESC subfamily of TTSPs that comprises HAT (encoded by TMPRSS11D), DESC1 (encoded by TMPRSS11E), HAT-like 4 (encoded by TMPRSS11F), HAT-like 5 (encoded by TMPRSS11B), and TMPRSS11A (encoded by TMPRSS11A) (Szabo and Bugge, 2011). Human HAT protein was first isolated in 1997 from the sputum of patients with chronic airway diseases and cloned the following year from human trachea cDNA (Yasuoka et al., 1997; Yamaoka et al., 1998). HAT is highly expressed in respiratory epithelium, where the protein localizes to the suprabasal layer of bronchial epithelium, as well as the basal region of their associated cilia. It has been proposed that HAT plays a role in mucus production (Takahashi et al., 2001; Chokki et al., 2004). In addition, it has been demonstrated that HAT supports proteolytic activation of influenza A and B viruses and the SARS coronavirus in vitro. Therefore, HAT may play a role in activation and spread of different respiratory viruses in the human airways (Böttcher-Friebertshäuser et al., 2010, 2013; Nygaard et al., 2011; Bertram et al., 2011; Baron et al., 2012). The expression of HAT transcript has been identified in several additional tissues including tongue, skin, esophagus, and cervix (Sales et al., 2011). While there has been an extensive body of literature documenting causal roles of TTSP

Competing interests: The authors declare that they have no competing interests.

Contract grant sponsor: Wayne State University School of Medicine.
Contract grant sponsor: Barbara Ann Karmanos Cancer Institute.
Contract grant sponsor: Kirschstein National Research Service Award;
Contract grant number: T32-CA009531.
Contract grant sponsor: NIGMS/NIH;
Contract grant number: R25 GM 058905-15.

*Correspondence to: Karin List, PhD, Department of Pharmacology and Oncology, Wayne State University School of Medicine, Gordon H. Scott Hall of Basic Medical Sciences, Room 6332, 540 East Canfield, Detroit, Michigan 48201.
E-mail: klist@med.wayne.edu

Manuscript Received: 11 March 2015
Manuscript Accepted: 21 August 2015

Accepted manuscript online in Wiley Online Library (wileyonlinelibrary.com): 22 August 2015.
DOI: 10.1002/jcp.25173

members in carcinogenesis, including hepsin, and matriptase (List, 2009; Antalis et al., 2010; Szabo and Bugge, 2011), HAT is one of the few family members that remains uncharacterized in cancer.

In this study, we performed a comprehensive expression analysis of HAT in cervical and esophageal tissues, and found that HAT was mainly localized on the surface of differentiated epithelial cells in healthy stratified squamous epithelia. In contrast, expression of the cell-surface protease is significantly diminished, and in many cases, undetectable in late stages of squamous cell carcinoma carcinogenesis.

Materials and Methods

Bioinformatics analysis

The Oncomine microarray database (http://www.oncomine.org) (Rhodes et al., 2004) was used to perform a meta-analysis of the expression of human *TMPRSS11d* (gene encoding the HAT protein) across two studies of the transcriptome in carcinomas of the cervix and esophagus as compared to normal control tissues (Table S1).

Ethics statement

The use of human tissue paraffin arrays was approved according to the institutional guidelines by the Wayne State University Institutional Review Board Administration (#2013-43).

Cell transfection

Human embryonic kidney cells, HEK293T, and human cervical carcinoma cells, HeLa (ATCC, Manassas, VA) were cultured in Dulbecco's modified Eagle's media (Gibco, Life Technologies, Grand Island, NY) supplemented with 10% fetal bovine serum (Atlanta Biologicals, Lawrenceville, GA). Full-length human HAT cDNA in pCAGGS was generously provided by Dr. Eva Friebertshaeuser, Philipps University Marburg. The generation of human full-length HATL-5 cDNA in pcDNA 3.1/V5-His TOPO® TA (Invitrogen, Life Technologies, Grand Island, NY) in frame with a C-terminal HIS-tag and V-5 epitope has previously been described (Miller et al., 2014). A control vector, pcDNA 3.1-GFP, was used to assess transfection efficiency and as a negative control for western blotting. Transfection of cells was performed using Lipofectamine LTX according to the manufacturer's instructions (Invitrogen, Life Technologies, Grand Island, NY). Transfections were performed with 2.5 μg plasmid DNA.

Western blotting

Cells were lysed using RIPA buffer: 150 mM NaCl, 50 mM Tris/HCl, pH 7.4, 0.1% SDS, 1% NP-40, and a protease inhibitor cocktail (Sigma–Aldrich, St. Louis, MO) and cleared by centrifugation at 12,000*g* at 4°C. For collection of conditioned media cells were serum starved overnight. Protein concentrations in whole cell lysates were determined using a Pierce BCA Protein Assay Kit (Thermo Scientific, Waltham, MA). Protein samples were separated by SDS-PAGE using 10% Tris-glycine gels under non-reducing or reducing conditions, transferred onto PVDF membranes (Bio-Rad Laboratories, Inc., Hercules, CA) and analyzed using rabbit anti human TMPRSS11d (HAT Ab1) (ab127031, Abcam, Cambridge, MA), rabbit anti human TMPRSS11d (HAT Ab2) (HPA052834 Sigma) or mouse anti V5 antibody (Invitrogen, Life Technologies, Grand Island, NY). For detection, secondary antibodies conjugated with horseradish peroxidase (Chemicon, Temecula, CA) were used in combination with ECL Western Blotting Substrate or Super-Signal West Femto Chemiluminescent Substrate (Pierce, Rockford, IL).

Tissue samples and immunohistochemistry

Cervical (CR802) and esophageal (ES482) tissue arrays including cancer and normal tissues as well as a universal normal tissue array (UNC241) were obtained from US Biomax, Inc. (Rockville, MD). Tissue arrays were deparaffinized with xylene and hydrated with graded ethanol solutions. Antigen retrieval was performed using citrate buffer, reduced pH, and endogenous peroxidases were quenched by incubating slides in 3% H_2O_2. The arrays were blocked with 2.5% bovine serum albumin (Sigma) in PBS, and incubated overnight at 4°C with 2 μg/ml rabbit anti human TMPRSS11d (HAT Ab1) (ab127031, Abcam, Cambridge, MA) or rabbit anti human TMPRSS11d (HAT Ab2) (HPA052834, Sigma) in a humidity chamber. All washing steps were performed using PBS. As a negative control, non-immune rabbit IgG (2 μg/ml) (NeoMarkers, Fremont, CA) was used. Bound antibodies were visualized using biotin-conjugated anti-rabbit (Vector Laboratories, Burlingame, CA) secondary antibodies, and a Vectastain ABC kit (Vector Laboratories, Burlingame, CA) or HRP conjugated Polymer Anti-Rabbit (Dako, Carpinteria, CA). 3,3′-diaminobenzidine (DAB) was used as the substrate (Sigma) and arrays were counterstained with hematoxylin. All microscopic images were acquired on a Zeiss Scope A.1 using digital imaging.

Evaluation of staining intensities and statistical analysis

Assessment of staining intensities of esophageal and cervical tissue samples was performed by manual assessment. Scores were assigned on the basis of the intensity and extent of epithelial staining in 20× microscopic fields using an arbitrary scale from 0 to 4 where: 0 = no epithelial cells stained; 1 = many epithelial cells stained weakly OR a few stained moderately with the majority unstained; 2 = the majority of epithelial cells stained weakly OR many epithelial cells stained moderately OR few epithelial cells stained strongly with the majority stained weakly or not at all; 3 = many epithelial cells stained strongly OR the majority stained moderately; and 4 = the majority of epithelial cells stained strongly. Statistical significance of the difference in HAT staining intensity between groups was determined by the two-tailed Mann–Whitney U test.

Results

Analysis of HAT protein expression in mammalian cells by western blotting

To minimize the risk of non-specific staining in immunohistochemical analysis (IHC) of tissue sections, we used two independent antibodies raised against different domains of the HAT protein. As illustrated in Figure 1A, the Ab1 antibody was raised against the serine protease (SP) domain, whereas the Ab2 antibody was raised against the stem region containing the SEA domain. The specificity of the two antibodies was tested in HEK293T and HeLa cells transfected with full-length human HAT cDNA. Western blot analysis under non-reducing conditions revealed a single band at the predicted molecular weight (46 kDa) (Yamaoka et al., 1998) with both antibodies in whole cell lysates from transfected HEK293T cells (Fig. 1B, left panels) and transfected HeLa cells (Fig. 1B, middle panel and data not shown). Since members of the HAT/DESC family display high homology, HEK293T, and HeLa cells transfected with V5-tagged full-length human HATL5 were included in the western blot analysis. None of the HAT antibodies showed cross-reactivity with HATL5 in HEK293T or HeLa cells (Fig. 1B, middle panel and data not shown). The presence of HATL5 protein in the lysates was confirmed using an anti-V5 antibody (Fig. 1B, right panel). Further analysis of whole cell lysates under reducing conditions was performed (Fig. 1C).

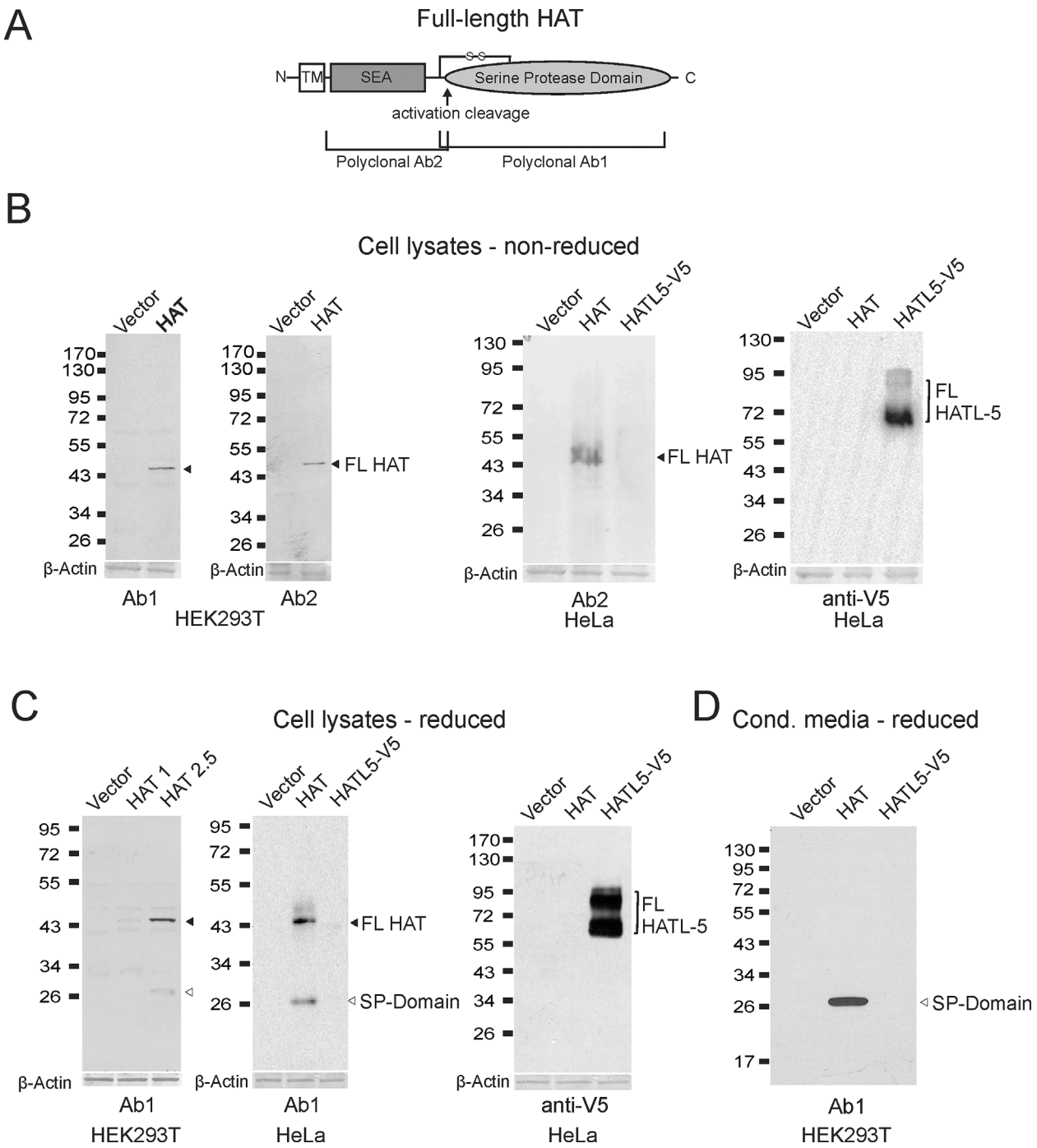

Fig. 1. Analysis of HAT protein expressed in mammalian cells. (A) Schematic representation of the HAT protein containing an N-terminal cytoplasmic tail, a transmembrane domain (TM), a stem region containing the SEA domain, and a C-terminal serine protease (SP) domain. The arrow indicates the activation cleaveage site between Arg^{186}-Ile^{187}. The stem region remains tethered to the serine protease domain by a disulfide bridge upon activation cleavage. The antigens used for generation of polyclonal antibodies Ab1 (serine protease domain) and Ab2 (SEA domain) are indicated. (B) Proteins from whole cell protein lysates were separated by SDS-PAGE under non-reducing conditions and analyzed by western blotting. HEK293T and HeLa cells were transfected with full-length human HAT, full-length V5-His tagged human HATL5 or a control vector containing GFP. Membranes were probed with HAT antibodies, Ab1 or Ab2 to visualized HAT protein, or anti-V5 to visualize HATL5 protein. The black arrowheads indicate the position of full-length (FL) 46 kDa form of HAT, and position of the glycosylated forms of full-length HATL-5 is indicated. Beta-actin staining of the membranes was performed to ensure equal protein loading. (C) Whole cell lysates were separated by SDS-PAGE under reducing conditions and analyzed by western blotting using Ab1 that recognizes the serine protease domain of HAT. The black arrowheads indicate the position of full-length (FL) HAT and the released serine protease (SP) domain is indicated with an open arrowhead. HEK293T cells were transfected with 1 μg and 2.5 μg HAT plasmid DNA as indicated. The position of the glycosylated forms of full-length HATL-5 is indicated on the blot probed with anti-V5. Beta-actin staining of the membranes was performed to ensure equal protein loading. (D) Serum-free conditioned media was collected and analyzed by SDS-PAGE under reducing conditions and western blotting. The position of the released serine protease (SP) domain is indicated by an open arrowhead.

TTSP's are synthesized as inactive zymogens that are activated by cleavage at a conserved activation site motif (predicted to be between Arg^{186}-Ile^{187} in HAT, indicated with an arrow in Fig. 1A). Upon activation, the catalytic domain remains tethered via a disulfide bond to the stem region of the protease. Therefore, the cleaved, active SP-domain can be visualized by SDS-PAGE and western blotting under reducing conditions using Ab1. As displayed in Figure 1C, the full-length form of HAT was detected in addition to a ~27 kDa form corresponding to the HAT SP-domain (Yasuoka et al., 1997) which was visible in both HEK293T and HeLa cells (left panels). Again, no cross-reactivity with HATL5 was detected. The V5 antibody readily detected HATL5 protein as expected (right panel). In conditioned media from HeLa cells (Fig. 1 D) and HEK293T cells (not shown), HAT was only detected as the 27 kDa form indicating that the majority of shed HAT is present in its active form.

HAT protein is localized on the cell surface of differentiated cells in stratified squamous epithelia

The TTSPs matriptase and TMPRSS13 play critical roles in terminal differentiation of squamous epithelia leading to the establishment of a functional barrier in the epidermis and oral cavity (List et al., 2002, 2003; Madsen et al., 2014). Interestingly, HAT mRNA is also expressed in several tissues containing squamous epithelia including skin, oral cavity, cervix, and esophagus (Sales et al., 2011). This prompted us to examine the distribution and cellular localization of HAT protein in squamous epithelia by IHC. The two independent anti-HAT rabbit antibodies raised against different HAT peptide antigens (Ab1 and Ab2) verified above were used to minimize the risk of non-specific staining. Using serial sections, slides were probed with primary antibodies or used as negative controls where the primary antibody was substituted with non-immune rabbit IgG (Fig. 2D, G and data not shown). Representative sections of

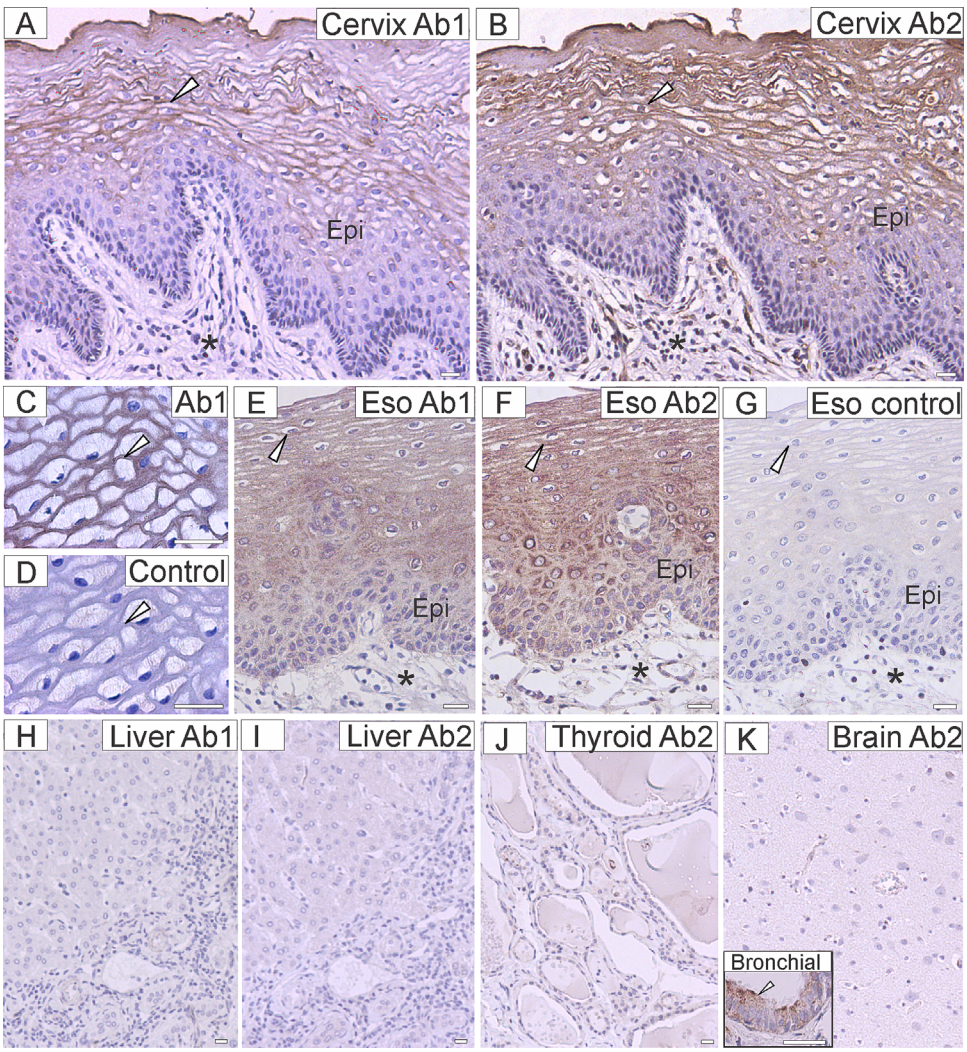

Fig. 2. Expression of HAT in cervix and esophagus. Immunohistochemical analysis of HAT expression in normal human squamous epithelia. HAT protein was detected with two different rabbit-anti HAT antibodies: HAT Ab1 (A, C, E) and HAT Ab2 (B, F). Primary antibodies were substituted with non-immune rabbit IgG in serial sections of all samples and no significant staining was observed (D, G and not shown). Strong epithelial staining (arrowheads) in apical, squamous epithelial cells in normal cervix is observed (A, B) with no significant staining in the mesenchymal compartment (indicated with asterisks). At high magnification, HAT protein is localized on the cell surface of apical epithelial cells (arrow head in C). In the esophagus, staining is observed in squamous suprabasal epithelium cells in addition to apical cells. (E, F). Epi=normal epithelium. No HAT expression is detected in liver (H, I), thyroid (J) or brain (K). Insert in K shows HAT staining in bronchial epithelium. Size bars all panels; 50 μm.

normal esophageal and cervical mucosa are shown in Figure 2. Careful inspection of staining patterns on serial sections revealed that the two anti-HAT antibodies displayed very similar staining pattern of the tissues examined (Fig. 2 A, B, E, F). In both the cervix and the esophagus, a strong epithelial staining was detected in the apical squamous cells with no significant staining in the submucosal or mesenchymal compartments. HAT protein is primarily localized on the cell surface of the larger squamous cells (Fig. 2C) and no nuclear staining was observed. This cell surface localization is in agreement with the expected distribution of the predicted membrane anchored topology of HAT. No significant staining was detected in the basal layer. The basal layers harbor the highly mitotic cells in in squamous epithelia (Huang et al., 2005; Looi et al., 2008). Sections from liver (Fig. 2H, I), thyroid (Fig. 2J) and brain (Fig.2 K), which have previously been shown to express no detectable HAT message by RT-PCR and Northern blot analysis (Yamaoka et al., 1998; Sales et al., 2011), were included as negative controls. The insert in Fig. 2K demonstrates HAT staining in bronchial epithelium as previously reported (Bertram et al., 2011). Taken together, these data demonstrate that endogenous HAT protein displays a pericellular localization in differentiating epithelial cells in stratified squamous epithelia.

Gradual loss of HAT expression in squamous cell carcinogenesis

Prior research has demonstrated the important roles of cell surface serine proteases in carcinogenesis. We first explored potential differential expression of HAT in normal and carcinomatous tissue by in silico data mining, using the Oncomine™ microarray database. Data analysis revealed a significant decrease in the overall level of HAT transcript in a meta-analysis of gene expression arrays studies of carcinomas from the cervix and esophagus as compared to corresponding normal tissues (Fig. 3A,B, Table S1). In order to gather a better understanding of the extent and localization of HAT protein expression in normal and cancerous tissue, we performed IHC using human tissue arrays composed of samples that varied in degree of pathogenicity from normal to poorly differentiated (Grade III) squamous cell carcinoma. Characteristics of squamous cell carcinoma progression include the presence of small and abnormally shaped cells with a loss of squamous appearance and a distinguishable basal membrane. Normal esophageal and cervical HAT protein expression was compared to squamous cell carcinoma of increasing grades using IHC analysis.

Cervical tissue arrays containing 21 normal cervical squamous epithelia samples and 28 cervical carcinoma samples with grades ranging from I to III (Grade I; n = 4, Grade II; n = 16, Grade III; n = 19) were incubated with the two different rabbit anti-HAT antibodies (Fig. 3C-F), and non-immune rabbit IgG as a negative control (not shown). Staining intensity was scored on a scale from 0 to 4 (Fig. 4A). Low-grade carcinomas (Grade I) showed moderate HAT membrane staining and weak cytoplasmic staining (Fig. 3C,D,L), whereas medium-grade carcinomas (Grade II), showed dispersed cytoplasmic expression with little or no cell surface staining (Fig. 3E,M). In poorly differentiated cervical carcinoma (Grade III), expression of HAT protease was largely absent, demonstrated by exceedingly weak or altogether absent cellular membrane and cytoplasmic staining (Fig. 3F). None of the samples displayed nuclear staining. In control samples where HAT antibody was replaced with non-immune rabbit IgG, staining could not be detected. Statistical analysis and comparison revealed a significant decrease in staining intensity in each of the two groups of cancer tissues Grade I–II ($P < 0.003$), and Grade III (0.00001), respectively, when compared to normal tissue (Fig. 4A).

Evaluation of differential expression of HAT in esophageal carcinoma was completed using normal and cancerous tissue samples with grades ranging from I to III (normal; n = 6, Grade I; n = 6, Grade II; n = 13, Grade III; n = 6). The esophageal tissue arrays were incubated with two different anti-HAT rabbit antibodies as described above (Fig. 3G, I, J,K and data not shown) and non-immune rabbit IgG as a negative control (Fig. 3H). In terms of HAT expression, well-differentiated, low-grade carcinomas (Grade I) showed moderately intense and dispersed cytoplasmic staining, while moderately differentiated carcinoma (Grade II) showed weak cytoplasmic dispersed expression with no visible cell surface staining. Three grade II tumors displayed no visible staining. In poorly differentiated carcinoma (Grade III), HAT expression was absent in two of the six samples, whereas the rest displayed faint to moderate HAT expression (Fig. 4B). Esophageal tissue arrays, incubated with non-immune rabbit IgG instead of HAT rabbit antibody, displayed no observable staining on the cell membranes, cytoplasm, or nucleus (Fig. 3M). Statistical analysis and comparison showed a significant decrease in staining intensity in Grade I ($P < 0.02$), Grade II ($P < 0.02$), and Grade III ($P < 0.01$) carcinomas in comparison to normal tissue (Fig. 4B).

Discussion

As part of an ongoing effort to determine the expression and function of the TTSP family in cancer, we performed expression analysis of HAT in healthy cervical and esophageal epithelia and in corresponding epithelia during squamous cell carcinogenesis. The specificity of the two HAT antibodies used in this study was verified by western blot analysis. Immunohistochemical analysis of HAT protein expression in human tissue arrays showed that the protease was consistently expressed in the suprabasal and apical layers harboring the most differentiated epithelial cells in healthy epithelia. The staining pattern in normal esophagus was consistent with that observed by Uhlén et al. (2015). Furthermore, HAT was mostly confined to the surface membrane of epithelial cells, consistent with the predicted localization of the type II transmembrane serine protease. Importantly, in squamous cell carcinomas of the same tissues, a significantly decreased expression and, in many cases, a complete loss of HAT was observed in advanced cancer. The localization of HAT protein in normal stratified squamous epithelia and the subsequent loss of the protease during carcinogenesis provide valuable information regarding the function of the protease in normal epithelial biology and carcinogenesis. In stratified squamous epithelia, a balance between cell proliferation, differentiation, and death must be carefully regulated in order to maintain their function. The stratified squamous epithelium acts as an effective barrier between the outside environments contaminants, including toxins and pathogens. The cells of these epithelia replicate frequently to replace damaged or dead cells. The proliferating epithelial cells reside in the basal layer and cells continuously pass through a complex differentiation program to generate basolateral and apical cells that are finally sloughed off (desquamation) at the surface of the epithelium. It has been demonstrated that extracellular proteases are involved in the acquisition of functional stratified squamous epithelia. Thus, the TTSPs, matriptase and TMPRSS13, are critical for terminal differentiation and proper function in the epidermis and oral epithelium (List et al., 2002, 2003; Madsen et al., 2014). Considering the finding that HAT is expressed in the non-proliferating suprabasal/apical layers combined with the observation that HAT is lost during the dedifferentiation of epithelial cells in high grade tumors, a hallmark of squamous cell carcinogenesis, an interesting question to explore further is

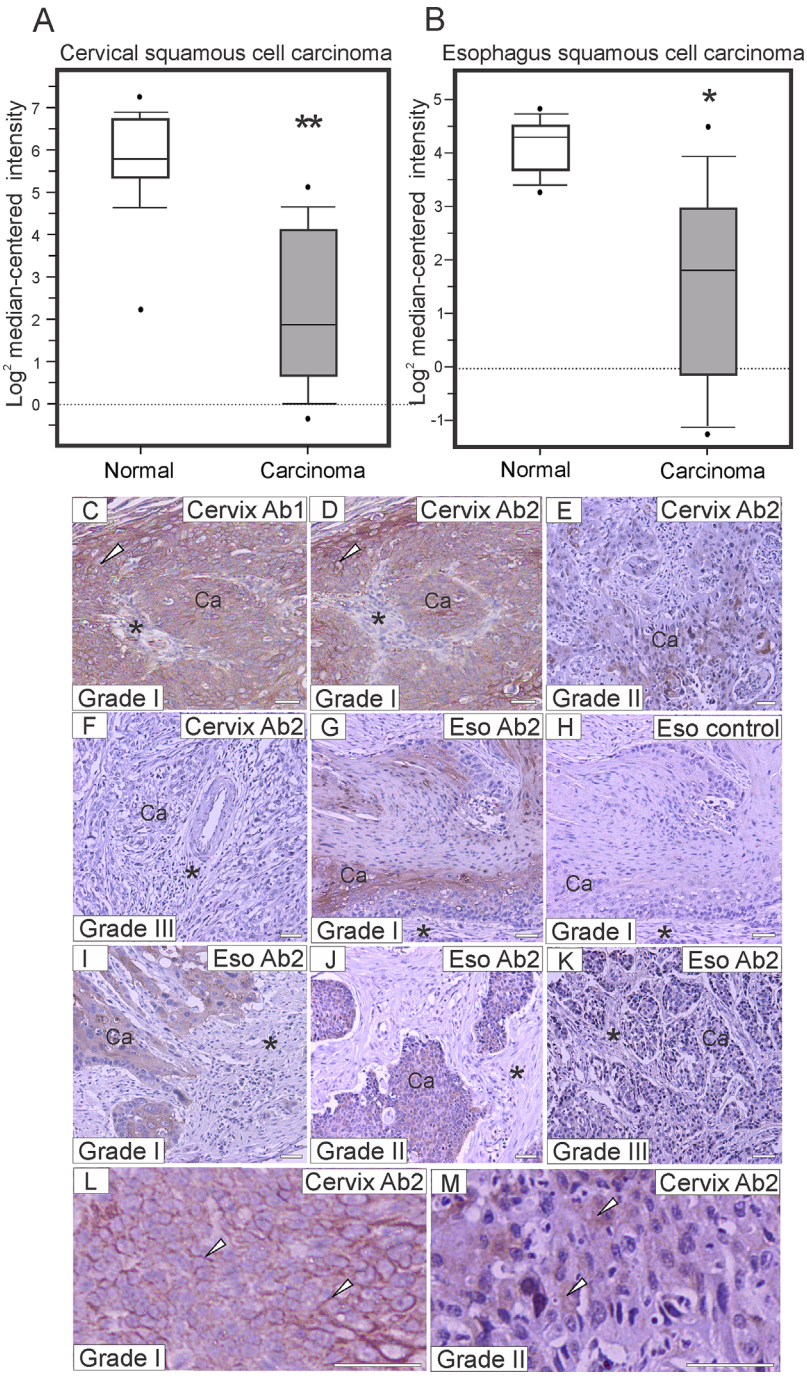

Fig. 3. Decreased expression of HAT protein in human carcinomas. (A,B) TMPRSS11d, encoding HAT in gene expression array studies of human squamous cell carcinoma of the cervix (study ID 1)(A) and esophagus (Study ID 2) (B) (see Table S1). HAT gene expression values in normal tissue (white bars) and carcinoma tissue (gray bars) are shown. The boxes show the interquartile range, the median is indicated by a vertical line and the black dots indicate maximum and minimum values. $^{*}P < 8 \cdot 10^{-6}$, $^{**}P < 7 \cdot 10^{-11}$. Samples sizes: cervix squamous epithelium (N = 21), cervical squamous cell carcinoma (N = 32); esophagus squamous epithelium (N = 17), esophageal squamous cell carcinoma (N = 17). (C–K) IHC detection of HAT protein in cervical tissue sections (C–F) and esophageal tissue sections (G–K). Primary antibodies were substituted with non-immune rabbit IgG in serial section of all samples and no significant staining was observed (H and not shown). Staining with two different rabbit anti-HAT antibodies (HAT Ab1 and Ab2) displayed similar staining patterns (C, D and not shown). In grade I cervical squamous carcinomas HAT staining was detected in the well-differentiated carcinoma cells (arrow heads in C, D) whereas weaker and more diffuse staining was observed in grade II cervical tumors (E). In high grade poorly differentiated tumors (Grade III) the staining intensity was low or below the detection limit of this assay (F). Stage I esophageal tumors displayed diffuse staining in carcinoma cells (G, I), and diffuse staining in some carcinoma cells were observed in Grade II tumors (J). In high grade poorly differentiated Grade III tumors the staining intensity was very low or below the detection limit of this assay (K). Epi=normal epithelium, Ca=carcinoma cells. (L) High magnification of grade I cervical squamous carcinoma to illustrate cell-surface localization of HAT and (M) grade III cervical squamous carcinoma where staining is primarily diffuse and intracellular. Size bars all panels; 50 μm.

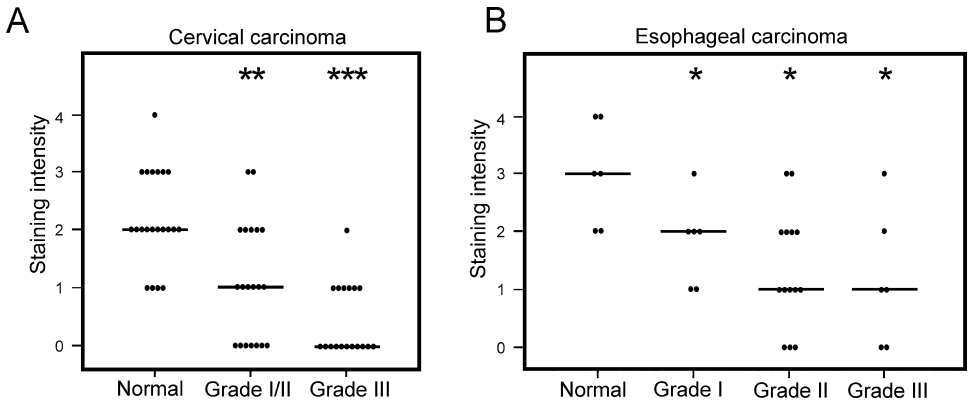

Fig. 4. Loss of HAT in esophageal and cervical carcinomas. Scatterplots illustrating the intensity of IHC staining of HAT in tissue array sections. Horizontal bars represent median values. Staining intensities were determined as described in "Materials and Methods." (A) In cervical squamous cell carcinoma, a highly significant decrease in staining intensity was observed between normal tissues and each of the two groups of cancer tissues divided according to Grade I–II ($P < 0.003$), and Grade III (0.00001), respectively. (B) In esophageal squamous cell carcinomas, a significant decrease in staining intensity was observed between normal tissues versus; grades I ($P < 0.02$), normal versus II ($P < 0.02$), and normal versus III ($P < 0.01$), respectively. Together, these data indicate a gradual loss of HAT expression during tumor progression in two types of squamous cell carcinoma.

whether the observed link between loss of HAT protein and squamous cell carcinoma progression is correlational or causal. A recent study demonstrated that HAT deficient mice did not display any overt phenotypes in the absence of external challenges or additional genetic deficits (Sales et al., 2011). However, it remains to be experimentally tested whether these mice have an altered susceptibility if subjected to e.g. chemical genotoxic stress or transgenic oncogene expression. Currently, the candidate endogenous mammalian proteolytic substrates identified for HAT include the urokinase receptor (uPAR), and the protease activated receptor (PAR) 2 (Iwakiri et al., 2004; Chokki et al., 2005; Matsushima et al., 2006; Beaufort et al., 2007; Liu et al., 2013). In addition, HAT has fibrinolytic activity and it has been hypothesized that HAT may participate in fibrinolysis within the airway mucous membranes, by cleaving fibrinogen transported from the blood stream (Yoshinaga et al., 1998). Interestingly, two other HAT/DESC subfamily members, DESC1 and HATL5 display similar expression patterns in normal stratified squamous epithelium and a gradual loss during carcinogenesis. Thus, DESC1 expression correlates with normal keratinocyte differentiation and inversely with head and neck squamous cell carcinoma progression (Lang and Schuller, 2001; Sedghizadeh et al., 2006). We have previously shown that HATL5 is significantly decreased in cervical, esophageal, and head and neck carcinomas as compared to normal tissue (Miller et al., 2014). An important finding in this connection is that cellular HAT is present in both its zymogen form and in its cleaved and active form and that shed HAT is present mainly in its active form upon transfection of full-length HAT cDNA in mammalian cells. Interestingly, the active forms of DESC1 or HATL5 were not detected in similar experiments (Hobson et al., 2004, Miller et al., 2014). Therefore it can be speculated that HAT acts as an activator and initiator of a proteolytic cascade during terminal differentiation of squamous epithelia similar to the proteolytic cascade of tissue kallikreins in the stratum corneum of the epidermis (Brattsand et al., 2005).

Conclusions

In summary, our current study represents a comprehensive expression characterization of HAT in healthy and cancerous tissues, and is a first step towards deciphering the potential functions of this protease in squamous cell carcinoma progression.

Authors' contributions

MJD and KL conceived the idea of the study. ASM carried out the Cancer Profiling Array analysis. MJD, GLZ and FAV optimized IHC and performed all the analysis of the tissue arrays. KOP, FAV, ASM, and MES performed cellular transfections and western blot analysis. MJD and KL wrote the manuscript. All authors contributed to interpretation and discussion of the results and read and approved the final version.

Acknowledgements

This work was supported by start-up funds from Wayne State University School of Medicine and Barbara Ann Karmanos Cancer Institute, Detroit, MI, NIH Ruth L. Kirschstein National Research Service Award T32-CA009531 (ASM), and NIGMS/NIH grant R25 GM 058905-15 (KOP, FAV). The funders had no role in study design, data collection and analysis, decision to publish, or preparation of the manuscript.

Literature Cited

Antalis TM, Buzza MS, Hodge KM, Hooper JD, Netzel-Arnett S. 2010. The cutting edge: Membrane-anchored serine protease activities in the pericellular microenvironment. Biochem 3:325–346.

Baron J, Tarnow C, Mayoli-Nüssle D, Schilling E, Meyer D, Hammami M, et al. 2012. Matriptase, HAT, and TMPRSS2 activate the hemagglutinin of H9N2 influenza A viruses. J Virol 87:1811–1820.

Beaufort N, Leduc D, Eguchi H, Mengele K, Hellmann D, Masegi T, Kamimura T, Yasuoka S, Fend F, Chignard M, Pidard D, Hellmann D. 2007. The human airway trypsin-like protease modulates the urokinase receptor (uPAR, CD87) structure and functions. Am J Physiol Lung Cell Mol Physiol 292:L1263–L1272.

Bertram S, Glowacka I, Müller MA, Lavender H, Gnirss K, Nehlmeier I, Niemeyer D, He Y, Simmons G, Drosten C, Soilleux EJ, Jahn O, Steffen I, Pöhlmann S. 2011. Cleavage and activation of the severe acute respiratory syndrome coronavirus spike protein by human airway trypsin-like protease. J Virol 85:13363–13372.

Brattsand M, Stefansson K, Lundh C, Haasum Y, Egelrud T. 2005. A proteolytic cascade of kallikreins in the stratum corneum. J Invest Dermatol 124:198–203.

Bugge TH, Antalis TM, Wu Q. 2009. Type II transmembrane serine proteases. J Biol Chem 35:23177–23181.

Böttcher-Friebertshäuser E, Freuer C, Sielaff F, Schmidt S, Eickmann M, et al. 2010. Cleavage of influenza virus hemagglutinin by airway proteases TMPRSS2 and HAT differs in subcellular localization and susceptibility to protease inhibitors. J Virol 84:5605–5614.

Böttcher-Friebertshäuser E, Klenk HD, Garten W. 2013. Activation of influenza viruses by proteases from host cells and bacteria in the human airway epithelium. Pathog Dis 69:87–100.
Chokki M, Yamamura S, Eguchi H, Masegi T, Horiuchi H, Tanabe H, Kamimura T, Yasuoka S. 2004. Human airway trypsin-like protease increases mucin gene expression in airway epithelial cells. Am J Respir Cell Mol Biol 30:470–478.
Chokki M, Eguchi H, Hamamura I, Mitsuhashi H, Kamimura T. 2005. Human airway trypsin-like protease induces amphiregulin release through a mechanism involving protease-activated receptor- 2-mediated ERK activation and TNF alpha-converting enzyme activity in airway epithelial cells. Febs J 272:6387–6399.
Hobson JP, Netzel-Arnett S, Szabo R, Réhault SM, Church FC, Strickland DK, Lawrence DA, Antalis TM, Bugge TH. 2004. Mouse DESC1 is located within a cluster of seven DESC1-like genes and encodes a type II transmembrane serine protease that forms serpin inhibitory complexes. J Biol Chem 45:46981–46994.
Huang JX, Yan W, Song ZX, Qian RY, Chen P, Salminen E, Toppari J. 2005. Relationship between proliferative activity of cancer cells and clinicopathological factors in patients with esophageal squamous cell carcinoma. World J Gastroenterol 11:2956–2959.
Iwakiri K, Ghazizadeh M, Jin E, Fujiwara M, Takemura T, Takezaki S, Kawana S, Yasuoka S, Kawanami O. 2004. Human airway trypsin-like protease induces PAR-2-mediated IL-8 release in psoriasis vulgaris. J Invest Dermatol 122:937–944.
Lang JC, Schuller DE. 2001. Differential expression of a novel serine protease homologue in squamous cell carcinoma of the head and neck. Br J Cancer 84:237–243.
List K, Haudenschild CC, Szabo R, Chen W, Wahl SM, Swaim W, Engelholm LH, Behrendt N, Bugge TH. 2002. Matriptase/MT-SP1 is required for postnatal survival, epidermal barrier function, hair follicle development, and thymic homeostasis. Oncogene 23:3765–3779.
List K, Szabo R, Wertz PW, Segre J, Haudenschild CC, Kim SY, Bugge TH. 2003. Loss of proteolytically processed filaggrin caused by epidermal deletion of Matriptase/MT-SP1. J Cell Biol 163:901–910.
List K. 2009. Matriptase: A culprit in cancer?. Future Oncol 1:97–104.
Liu C, Li Q, Zhou X, Kolosov VP, Perelman JM. 2013. Human airway trypsin-like protease induces mucin5AC hypersecretion via a protease-activated receptor 2-mediated pathway in human airway epithelial cells. Arch Biochem Biophys 535:234–240.
Looi ML, Dali AZ, Ali SA, Ngah WZ, Yusof YA. 2008. Expression of p53, bcl-2 and Ki-67 in cervical intraepithelial neoplasia and invasive squamous cell carcinoma of the uterine cervix. Anal Quant Cytol Histol 30:63–70.
Madsen DH, Szabo R, Molinolo AA, Bugge TH. 2014. TMPRSS13 deficiency impairs stratum corneum formation and epidermal barrier acquisition. Biochem J 461:487–495.
Matsushima R, Takahashi A, Nakaya Y, Maezawa H, Miki M, Nakamura Y, Ohgushi F, Yasuoka S. 2006. Human airway trypsin-like protease stimulates human bronchial fibroblast proliferation in a protease-activated receptor-2-dependent pathway. Am J Physiol Lung Cell Mol Physiol 290:L385–L395.
Miller GS, Zoratti GL, Murray AS, Bergum C, Tanabe LM, List K. 2014. HATL5: A cell surface serine protease differentially expressed in epithelial cancers. PLoS One 9:e87675.
Nygaard RM, Golden JW, Schiff LA. 2011. Impact of host proteases on reovirus infection in the respiratory tract. J Virol 86:1238–1243.
Rhodes DR, Yu J, Shanker K, Deshpande N, Varambally R, Ghosh D, Barrette T, Pandey A, Chinnaiyan AM. 2004. ONCOMINE: A cancer microarray database and integrated data-mining platform. Neoplasia 1:1–6.
Sales KU, Hobson JP, Wagenaar-Miller R, Szabo R, Rasmussen AL, Bey A, Shah MF, Molinolo AA, Bugge TH. 2011. Expression and genetic loss of function analysis of the HAT/DESC cluster proteases TMPRSS11A and HAT. PLoS One 6:23261.
Sedghizadeh PP, Mallery SR, Thompson SJ, Kresty L, Beck FM, Parkinson EK, Biancamano J, Lang JC. 2006. Expression of the serine proteases DESC1 correlates directly with normal keratinocyte differentiation and inversely with head and neck squamous cell carcinoma progression. Head Neck 28:432–440.
Szabo R, Bugge TH. 2008. Type II transmembrane serine proteases in development and disease. Int J Biochem Cell Biol 40:1297–1316.
Szabo R, Bugge TH. 2011. Membrane-anchored serine proteases in vertebrate cell and developmental biology. Annu Rev Cell Dev Biol 27:213–235.
Takahashi M, Sano T, Yamaoka K, Kamimura T, Umemoto N, Nishitani H, Yasuoka S. 2001. Localization of human airway trypsin-like protease in the airway: An immunohistochemical study. Histochem Cell Biol 115:181–187.
Uhlén M, Fagerberg L, Hallström BM, Lindskog C, Oksvold P, Mardinoglu A, Sivertsson A, Kampf C, Sjöstedt E, Asplund A, Olsson I, Edlund K, Lundberg E, Navani S, Szigyarto CA, Odeberg J, Djureinovic D, Takanen JO, Hober S, Alm T, Edqvist PH, Berling H, Tegel H, Mulder J, Rockberg J, Nilsson P, Schwenk JM, Hamsten M, von Feilitzen K, Forsberg M, Persson L, Johansson F, Zwahlen M, von Heijne G, Nielsen J, Pontén F. 2015. Proteomics. Tissue-based map of the human proteome. Science 347:1250419.
Yasuoka S, Ohnishi T, Kawano S, Tsuchihashi S, Ogawara M, Masuda K, Yamaoka K, Takahashi M, Sano T. 1997. Purification, characterization, and localization of a novel trypsin-like protease found in the human airway. Am J Respir Cell Mol Biol 16:300–308.
Yamaoka K, Masuda K, Ogawa H, Takagi K, Umemoto N, Yasuoka S. 1998. Cloning and characterization of the cDNA for human airway trypsin-like protease. J Biol Chem 273:11895–11901.
Yoshinaga S, Nakahori Y, Yasuoka S. 1998. Fibrinogenolytic activity of a novel trypsin-like enzyme found in human airway. J Med Invest 45:77–86.

Supporting Information

Additional supporting information may be found in the online version of this article at the publisher's web-site.